



OPEN ACCESS

EDITED BY

Qi Dai,
Zhejiang Sci-Tech University, China

REVIEWED BY

Zhuoxing Shi,
Zhongshan Ophthalmic Center, Sun
Yat-sen University, China
Lei Chen,
Shanghai Maritime University, China

*CORRESPONDENCE

Shengyu Li,
doctorlsy@126.com
Xiaofeng Li,
lixiaofeng878@163.com

SPECIALTY SECTION

This article was submitted to Genetics of
Common and Rare Diseases,
a section of the journal
Frontiers in Genetics

RECEIVED 07 August 2022

ACCEPTED 09 November 2022

PUBLISHED 25 November 2022

CITATION

Li S, Liu Y, Liu M, Wang L and Li X (2022),
Comprehensive bioinformatics analysis
reveals biomarkers of DNA methylation-
related genes in varicose veins.
Front. Genet. 13:1013803.
doi: 10.3389/fgene.2022.1013803

COPYRIGHT

© 2022 Li, Liu, Liu, Wang and Li. This is
an open-access article distributed
under the terms of the [Creative
Commons Attribution License \(CC BY\)](#).
The use, distribution or reproduction in
other forums is permitted, provided the
original author(s) and the copyright
owner(s) are credited and that the
original publication in this journal is
cited, in accordance with accepted
academic practice. No use, distribution
or reproduction is permitted which does
not comply with these terms.

Comprehensive bioinformatics analysis reveals biomarkers of DNA methylation-related genes in varicose veins

Shengyu Li^{1*}, Yuehan Liu², Mingming Liu¹, Lizhao Wang¹ and Xiaofeng Li^{1*}

¹Department of Vascular Surgery, Tianjin First Central Hospital, Tianjin, China, ²Department of Functional Examination, Beijing Aerospace General Hospital, Beijing, China

Background: Patients with Varicose veins (VV) show no obvious symptoms in the early stages, and it is a common and frequent clinical condition. DNA methylation plays a key role in VV by regulating gene expression. However, the molecular mechanism underlying methylation regulation in VV remains unclear.

Methods: The mRNA and methylation data of VV and normal samples were obtained from the Gene Expression Omnibus (GEO) database. Methylation-Regulated Genes (MRGs) between VV and normal samples were crossed with VV-associated genes (VVGs) obtained by weighted gene co-expression network analysis (WGCNA) to obtain VV-associated MRGs (VV-MRGs). Their ability to predict disease was assessed using receiver operating characteristic (ROC) curves. Biomarkers were then screened using a random forest model (RF), support vector machine model (SVM), and generalized linear model (GLM). Next, gene set enrichment analysis (GSEA) was performed to explore the functions of biomarkers. Furthermore, we also predicted their drug targets, and constructed a competing endogenous RNAs (ceRNA) network and a drug target network. Finally, we verified their mRNA expression using quantitative real-time polymerase chain reaction (qRT-PCR).

Results: Total three VV-MRGs, namely Wnt1-inducible signaling pathway protein 2 (WISP2), Cysteine-rich intestinal protein 1 (CRIP1), and Odd-skipped related 1 (OSR1) were identified by VVGs and MRGs overlapping. The area under the curves (AUCs) of the ROC curves for these three VV-MRGs were greater than 0.8. RF was confirmed as the optimal diagnostic model, and WISP2, CRIP1, and OSR1 were regarded as biomarkers. GSEA showed that WISP2, CRIP1, and OSR1 were associated with oxidative phosphorylation, extracellular matrix (ECM), and respiratory system functions. Furthermore, we found that lncRNA MIR17HG can regulate OSR1 by binding to hsa-miR-21-5p and that PAX2 might treat VV by targeting OSR1. Finally, qRT-PCR results showed that the mRNA expression of the three genes was consistent with the results of the datasets.

Conclusion: This study identified WISP2, CRIP1, and OSR1 as biomarkers of VV through comprehensive bioinformatics analysis, and preliminary explored the

DNA methylation-related molecular mechanism in VV, which might be important for VV diagnosis and exploration of potential molecular mechanisms.

KEYWORDS

varicose veins, DNA methylation, machine learning, biomarkers, bioinformatics

Introduction

Varicose veins (VV) are a common manifestation of chronic venous disease, commonly affecting the lower extremities, causing twisted and dilated veins (Fukaya et al., 2018; Raetz et al., 2019). Approximately 25% of adults suffer from varicose veins (Li et al., 2014). VV can cause systemic symptoms, such as aching, heaviness, cramping, throbbing, restlessness, and swelling in the legs (Gloviczki et al., 2011). The exact pathophysiological mechanism of VV remains controversial but might be related to genetic predispositions, defects in the valves, weakening of the vascular walls, and high intravenous pressure (Raetz et al., 2019). VV is sometimes dismissed as a mere cosmetic issue, but in 20% of patients, it can lead to life-threatening ulcers (Beebe-Dimmer et al., 2005). According to recent studies, patients with VV are up to 5-fold more likely to develop deep vein thrombosis. In addition, it may lead to peripheral arterial disease (Chang et al., 2018). There is an economic burden on the society because varicose diseases have serious consequences. In the United States, more than 30 million adults suffer from VV, resulting in direct medical costs of over \$ 1 billion annually (Gloviczki et al., 2011). Therefore, it is important to understand the molecular mechanism underlying VV and to identify potential biomarkers and drug targets that are likely to be effective in preventing it.

DNA methylation is the most prevalent DNA modification and plays an important role in both eukaryotic and prokaryotic life processes (Yang et al., 2020). As an epigenetic mechanism, it can influence gene expression through processes that affect DNA structure and stability, and chromatin structure (Kundu and Peterson, 2009; Jiang et al., 2014). Furthermore, DNA methylation is the main epigenetic form of gene expression regulation in mammals (Huang et al., 2015), mostly occurring on CpG islands in the gene promoter region, where methylation can repress gene transcription (Qin et al., 2015). Studies have shown that DNA methylation status might be involved in the regulation of atherogenesis, diabetes, inflammation, and hypertension (Friso et al., 2008; Ling and Groop, 2009; Turunen et al., 2009). Smetanina et al. (2018) delivered new viewpoints that MFAP5 might play an important role in VV as a master regulator. At meantime, the study provided a preliminary evidence that DNA methylation critically effected on the initiation and progression of VV through function enrichment and systems biology analyses. It was the first study combining OMIC data, including transcriptomics and methylation data, to study the mechanism of VV pathogenesis. Based on the results, we further explored the DNA methylation-related molecular mechanism in VV

with same datasets using comprehensive bioinformatics analysis. Besides, whole transcriptome data from 45 samples in GSE36809 dataset were first extracted to analyze the relationship between biomarkers and related miRNA, lncRNA in VV (Xiao et al., 2011; Seok, 2015).

Machine learning can train computers to perform tasks by identifying patterns in massive datasets to determine the rules or algorithms that optimize task completion (Lynch and Liston, 2018). Machine learning has been reported to predict secondary structural features of proteins (Wang et al., 2021) and facilitate the discovery of biomarkers for predicting diseases (Kourou et al., 2015; Lynch and Liston, 2018). It is also widely used in the prognosis and diagnosis of a variety of diseases (Wang and Huang, 2011; Kourou et al., 2015), such as in Yang's research, machine learning can predict the carcinogenic or non-carcinogenic risk genotype of unknown HPV (Yang et al., 2022). Therefore, machine learning can be used to explore biomarkers of VV.

In this study, DNA methylation-related molecular mechanism in VV was investigated for the first time through the comprehensive bioinformatics analyses on transcriptome data, and the biomarkers of VV (WISP2, CRIP1, and OSR1) were identified using three machine learning models. Furthermore, a biomarkers-related lncRNA-miRNA-mRNA-drug network was predicted, which might provide a reference for clinical research and treatment of VV.

Materials and methods

Data collection

In this study, mRNA expression and methylation data of VV and normal samples were obtained from the Gene Expression Omnibus (GEO) database (<https://www.ncbi.nlm.nih.gov/geo/>). The mRNA expression data of seven VV and seven normal samples were obtained from the GSE68309 dataset, while the GSE68319 dataset contained methylation data of seven VV samples and seven normal samples the patient sources for the GSE68319 and GSE68309 datasets were the same. In addition, whole transcriptome data of 45 blood samples were acquired from the GSE36809 dataset.

Identification of differentially methylated CpGs sites

DMCs were obtained by comparing the methylation sites of VV and normal samples in the GSE68319 dataset using the

“ChAMP” (version 2.20.1) R package with a screening condition of $p < 0.05$ (Tian et al., 2017). The “Rideoogram” R package (version 0.2.2) was then used to visualize the chromosome annotation information of DMCs (Hao et al., 2020). Finally, we compared the distribution of CpG sites in different regions within genes to obtain differentially methylated regions (DMRs) using the “UpSetR” (version 1.4.0) R package (Conway et al., 2017).

Functional enrichment analysis of methylation-regulated genes

In the GSE68309 dataset, differentially expressed genes (DEGs) between VV and normal samples were compared using the “edgeR” (version 3.34.1) R package with the screening condition of $|\log_2FC| > 0.5$, $p < 0.05$ (Robinson et al., 2010). The expression of DEGs was shown by the volcano plot drawn by the “ggplot2” R package (version 3.3.5) (Zhang and Wang, 2022). We then corresponded DMCs to the corresponding genes based on methylation annotation information, and the methylation levels were upregulated for hypermethylated genes and downregulated for demethylated. MRGs were obtained from the intersections of the demethylated and highly expressed genes as well as the hypermethylated and the low-expressed genes. The enrichment analysis of Kyoto Encyclopedia of Genes and Genomes (KEGG) and Gene ontology (GO) was performed using “clusterProfiler” R package (Version 4.0.2) to find the functions and related pathways of the MRGs with the significance threshold of $p < 0.05$ (Yu et al., 2012).

Identification of diagnostic genes

Weighted gene co-expression network analysis (WGCNA) can cluster modules by gene expression similarity and screen modules with highly correlated traits based on the correlations between modules and traits to find target genes (Langfelder and Horvath, 2008). In this study, we used normal and VV samples as trait data. Total seven normal and seven VV samples in the GSE68309 dataset were used as trait data for WGCNA using the “WGCNA” R package (version 1.70-3) to identify VV-associated genes (VVGs). First, the samples were clustered to determine whether outlier samples needed to be removed. Based on the clinical trait information, sample clustering and clinical trait heat maps were subsequently drawn. To ensure that the interactions between genes maximally conformed to a scale-free distribution, we determined the soft threshold. Based on the optimal soft threshold, we set the minimum number of genes per gene module to 100 and the cutting height to $MEDissThres = 0.7$, according to the criteria of the hybrid dynamic tree cutting algorithm, to draw the module clustering tree. The modules significantly associated

with VV were then identified as key modules based on their correlations with the traits. Finally, scatter plots were drawn for key modules to show the correlations between genes and modules (Module Membership, MM) and between genes and traits (Gene Significance, GS), with the threshold values: $|GS| > 0.5$, $|MM| > 0.7$, and $p \leq 0.05$ to screen VVGs. The VVGs were then intersected with the MRGs to obtain VV-associated MRGs (VV-MRGs). To assess the disease prediction ability of VV-MRGs, receiver operating characteristic (ROC) curve was plotted by the “pROC” (version 1.18.0) R package (Robin et al., 2011). The area under the curve (AUC) value refers to the area under the ROC curve. The larger the value, the more accurate is the prediction. VV-MRGs with AUC values > 0.8 were used as diagnostic genes.

Identification of biomarkers by machine learning algorithms

To screen biomarkers, we calculated the importance of diagnostic genes using three machine learning methods: random forest model (RF), support vector machine model (SVM), and generalized linear model (GLM) (Qu et al., 2022; Wang et al., 2022). The models were analyzed using the “DALEX” R package (version 2.3.0) to plot residual distributions, and algorithmic power box line plots to obtain the best model from which biomarkers were obtained (Floyd et al., 2022). The nomogram of biomarkers was constructed using the “RMS” (version 6.1-0) R package to derive the relationship between biomarkers and diseases, and the calibration curves plotted by “RMS” (version 6.1-0) R package were used to validate the model (Qiu et al., 2022).

Gene set enrichment analysis of biomarkers

To further investigate the relevant signaling pathways and potential biological mechanisms in VV samples, we used the “clusterProfiler” (version 3.18.1) and the “org.Hs.eg.db” (version 3.12.0) R packages to perform single-gene GO and KEGG enrichment analyses for the diagnostic genes (Li et al., 2021). The median expression values of the diagnostic genes were used to classify the samples into high- and low-risk groups. GSEA enrichment analysis was then performed for all genes, with the threshold set at $|NES| > 1$, $p < 0.05$, and $q < 0.25$ (Subramanian et al., 2005).

Competing endogenous RNA and drug target networks

We downloaded the drug targets from the binding database. We then constructed a protein-protein interaction (PPI) network

TABLE 1 Primers used for reverse transcription-quantitative PCR.

Sequence name	Forward primer (5'-3')	Reverse primer (3'-5')
WISP2	CTGGATGGCTGTGGCT	AACTGGGGTCCTTGGG
OSR1	AGTGGACGCTGGGCTA	GGGCTTGGGTTGAATG
CRIP1	AAATGTGGGAAGACGCT	GGTGGTTGCAGTAGGGT
GAPDH	CCCATCACCATCTTCCAGG	CATCACGCCACAGTTTCCC

between drug targets and biomarkers based on the STRING database (von Mering et al., 2003), and selected drug targets with an interaction score >0.7. In order to investigate the relationship for gene expression of biomarkers with targeting miRNA and corresponding lncRNA, the relative information from 45 blood samples within GSE36809 dataset was extracted. We searched for miRNAs related to biomarkers from the miRwalk and miRDB databases (Liu et al., 2020), merged the results of the two databases, and obtained candidate miRNAs interacting with biomarkers (mRNAs). Next, we searched for miRNAs that crossed with the candidate miRNAs in the GSE36809 dataset, and used the “tidyr” (version 1.1.4) R package to calculate the correlations between biomarkers (mRNAs) and miRNAs (Mangiola et al., 2021). Furthermore, we used miRNAs to predict the lncRNAs in the Starbase database (Li et al., 2014). Finally, mRNA-miRNA and miRNA-lncRNA were obtained based on the above analysis, and a ceRNA network was constructed using Cytoscape software (Shannon et al., 2003). The lncRNA-miRNA-mRNA-drug network was also constructed based on the potential therapeutic drugs identified in the previous step.

Quantitative real-time polymerase chain reaction validation

Seven patients with VV were recruited from Tianjin First Central Hospital. The study met the ethical requirements of Tianjin First Central Hospital. Samples from diseased and normal venous vessels of VV were taken from the participants, and RNA was extracted using TRIzol Reagent (REF:15596018) provided by Ambion. Reverse transcription was performed using the sweScript RT I First strand cDNA Synthesis All-in-One™ Kit (REF:15596018) (Servicebio Technology Co., Ltd., in Wuhan, Hubei Province, China). PCR was performed using the 2xUniversal Blue SYBR Green qPCR Master Mix (CAT-G3326-05) kit (Servicebio Technology Co., Ltd., in Wuhan, Hubei Province, China) (Bachman, 2013). The PCR conditions were as follows: pre-denaturation at 95°C for 1 min followed by 40 cycles, each of denaturation at 95°C for 20 s, 55°C for 20 s, and extension at 72°C for 30 s. GAPDH was used as an internal reference for gene detection. Primer sequences are shown in Table 1. The expressions of WISP2, OSR1, and

CRIP1 in diseased and normal venous vessels were compared by analysis of variance (ANOVA), and $p < 0.05$ was considered as significant.

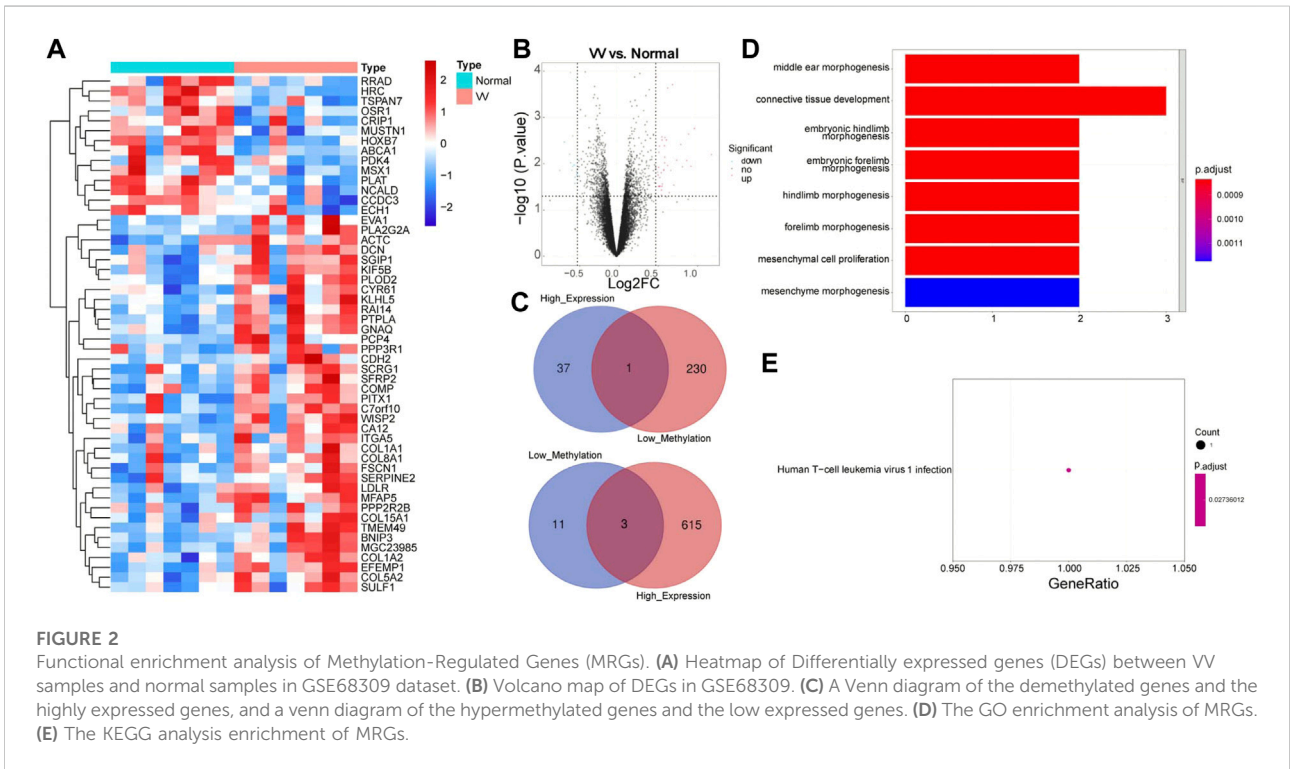
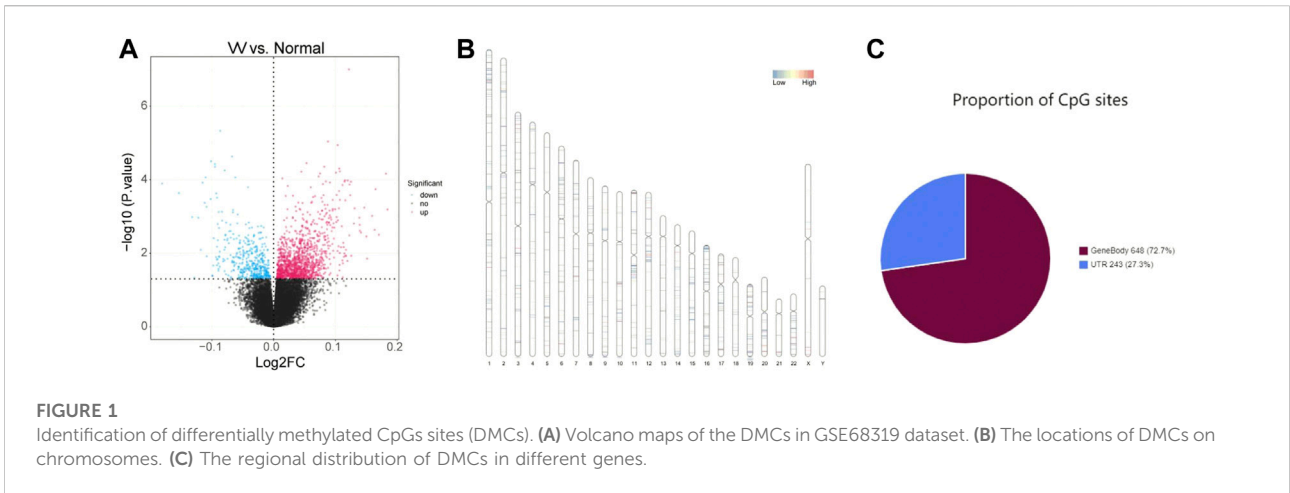
Results

Identification of differentially methylated CpGs sites

The whole flowchart of the study was shown in Supplementary Figure S1. Total 1645 DMCs were screened between VV and normal samples, including 1208 upregulated and 437 downregulated sites, and the results are shown in Supplementary Table S1. Volcano maps were drawn based on the DMCs (Figure 1A). There were 891 CpG sites with annotation information, and Figure 1B shows the locations of the DMCs on the chromosomes. The regional distribution of DMCs in the different genes is shown in Figure 1C. Most (72.7%) of the CpG sites were located within the gene.

Functional enrichment analysis of methylation-regulated genes

In the GSE68309 dataset, 52 DEGs were screened out between VV and normal samples, including 38 upregulated and 14 downregulated DEGs (Supplementary Table S2). Volcano and heat maps of DEGs were shown in Figures 2A,B. The demethylated and the highly expressed genes as well as the hypermethylated and the low expressed genes were intersected to obtain four MRGs: WISP2, OSR1, MSX1, and CRIP1, which are shown in Figure 2C. We then annotated the above four MRGs using the KEGG pathway and GO function to explore the biological significance of each gene. A total of 201 GOs and one KEGG pathway were enriched, as shown in Supplementary Table S3. Figure 2D showed the enrichment of the top eight GOs: middle ear morphogenesis, connective tissue development, embryonic hindlimb morphogenesis, embryonic forelimb morphogenesis, hindlimb morphogenesis, forelimb morphogenesis, mesenchymal cell proliferation, and mesenchyme morphogenesis. KEGG enrichment was shown in Figure 2E, and its pathway has been determined to be Human T-cell leukemia virus 1 infection.



Identification of diagnostic genes

The sample clustering plot showed that there were no outlier samples in the GSE68309 dataset (Figure 3A). The sample clustering and clinical trait heat map showed that the VV and normal samples were clustered well (Figure 3B). The network approximated a scale-free distribution when the power threshold was four (Figure 3C). A total of 23 modules were segmented by the hybrid dynamic shear tree algorithm, and 11 modules were obtained after merging, and the module clustering tree was

shown in Figure 3D. The correlations between MODULE and grouped traits were shown in Figure 3E. Among the 11 modules, the brown module ($R^2 = 0.53, p = 0.05$) had a high and significant positive correlation with VV. Therefore, the brown module was identified as the key module, with 18631 genes. The MM and GS scatter plots of the brown module were shown in Figure 3F, and 126 VVGs were obtained (Supplementary Table S4). The intersection of VVGs and MRGs was used to obtain three VV-MRGs: WISP2, CRIP1, and OSR1 (Figure 3G). As shown in Figure 3H, the AUC values for WISP2, CRIP1, and OSR1 were

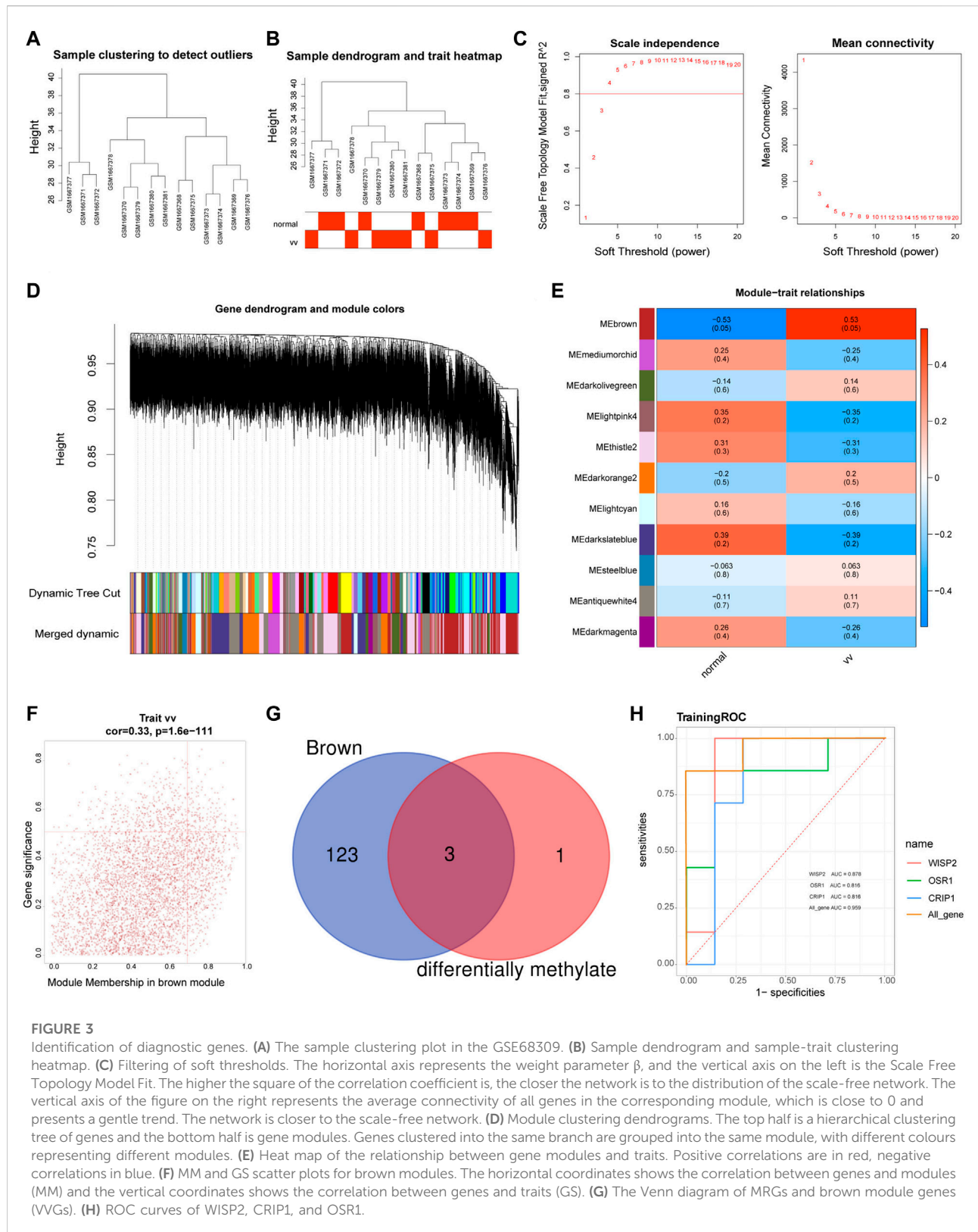
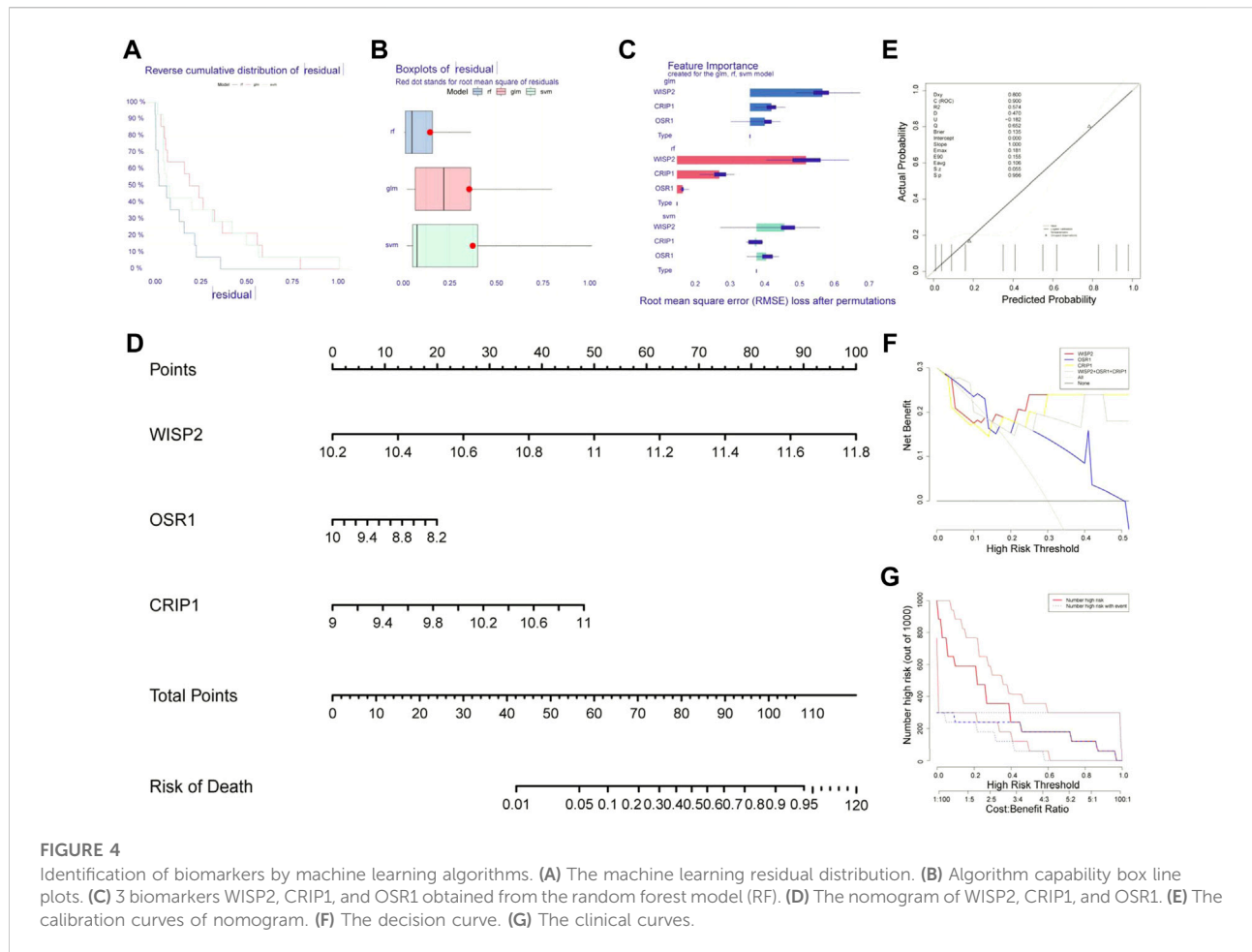


FIGURE 3

Identification of diagnostic genes. (A) The sample clustering plot in the GSE68309. (B) Sample dendrogram and sample-trait clustering heatmap. (C) Filtering of soft thresholds. The horizontal axis represents the weight parameter β , and the vertical axis on the left is the Scale Free Topology Model Fit. The higher the square of the correlation coefficient is, the closer the network is to the distribution of the scale-free network. The vertical axis of the figure on the right represents the average connectivity of all genes in the corresponding module, which is close to 0 and presents a gentle trend. The network is closer to the scale-free network. (D) Module clustering dendrograms. The top half is a hierarchical clustering tree of genes and the bottom half is gene modules. Genes clustered into the same branch are grouped into the same module, with different colours representing different modules. (E) Heat map of the relationship between gene modules and traits. Positive correlations are in red, negative correlations in blue. (F) MM and GS scatter plots for brown modules. The horizontal coordinates shows the correlation between genes and modules (MM) and the vertical coordinates shows the correlation between genes and traits (GS). (G) The Venn diagram of MRGs and brown module genes (VVGs). (H) ROC curves of WISP2, CRIP1, and OSR1.



0.878, 0.816, and 0.816, respectively. Moreover, their combined AUC was 0.905 and displayed excellent diagnostic performance.

Identification of biomarkers by machine learning algorithms

The machine learning residual distribution and algorithm capability box line plots were shown in Figures 4A,B, where the RF algorithm outperformed the SVM and GLM algorithms. We then obtained three biomarkers, WISP2, CRIP1, and OSR1, from RF (Figure 4C). The biomarker nomogram was shown in Figure 4D. The calibration curves were plotted in Figure 4E. The results showed that the model passed the calibration degree test with $p > 0.05$, and the ROC area was 0.900 with good discriminatory ability. Overall, the predictive ability of the model was excellent. The decision curve graph showed that the net benefit of all three biomarkers was higher than that of individual biomarkers (Figure 4F). The clinical curves showed that the biomarkers were better predictors of prognosis (Figure 4G).

Gene set enrichment analysis enrichment analysis of biomarkers

First, the WISP2 diagnostic gene was used for single-gene GSEA enrichment analysis, and 262 GO enrichment profiles and 27 KEGG pathways were obtained, including extracellular structure tissue, collagen fibril tissue, collagen-containing ECM and its structural components, focal adhesion, and receptor interactions (Supplementary Tables S5, S6; Figures 5A,B). Single-gene GSEA enrichment analysis was also conducted with the CRIP1 diagnostic gene, and 178 GO enrichment conditions and 21 KEGG pathways were obtained, including external encapsulating structure organization, oxidative phosphorylation, respiratory system, organelle inner membrane, structural components of ECM, structural components of ribosomes, and ECM receptor interactions, etc. (Supplementary Tables S7, S8; Figures 5C,D). OSR1 diagnostic gene was used for single-gene GSEA enrichment analysis, and 206 GO enrichment conditions and 24 KEGG pathways were obtained, including external encapsulating structure organization, collagen fiber organization, cell organelle internal membrane, respiratory system, metabolism of

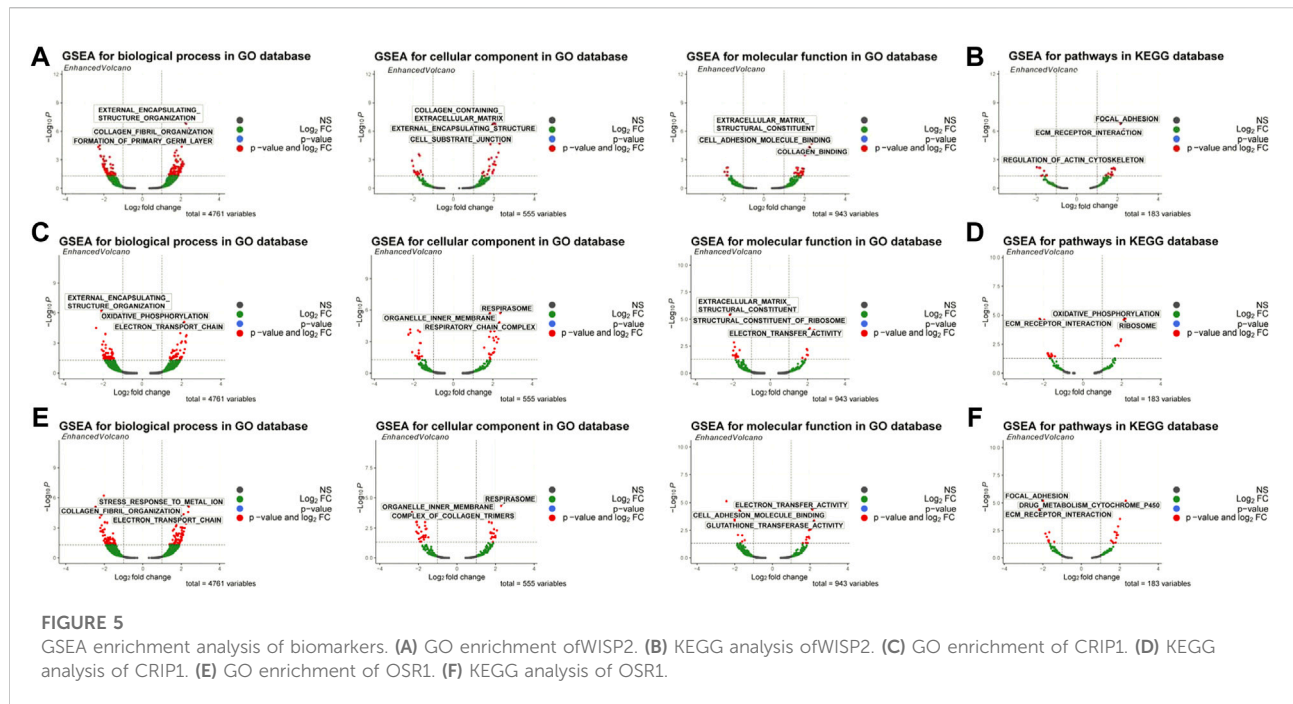


FIGURE 5
GSEA enrichment analysis of biomarkers. (A) GO enrichment of WISP2. (B) KEGG analysis of WISP2. (C) GO enrichment of CRIP1. (D) KEGG analysis of CRIP1. (E) GO enrichment of OSR1. (F) KEGG analysis of OSR1.

toxic substances by cytochrome p450, ECM structure components that constitute tensile strength, electron transfer activity (Supplementary Tables S9, S10; Figures 5E,F).

Competing endogenous RNA and drug target networks

A total of 12 drug targets were obtained, of which two were high-scoring targets. Specifically, the WISP2 gene predicted LRP5, HDAC1, IGF1, WNT2, and CTNBN1 drug targets, the CRIP1 gene predicted STK3, STK4, CBF, and DBI drug targets, and the OSR1 gene predicted VHL, PAX2, and EGLN1 drug targets, among which, STK3 and STK4 were high-scoring drug targets (Figure 6A). The miRNAs associated with the biomarkers in the miWalk and miRDB databases were merged to obtain 513 candidate miRNAs (Figure 6B). We identified 26 miRNAs in the GSE36809 dataset. Based on the ceRNA network, miRNA and mRNA expressions were negatively correlated, and three miRNAs with negative correlations were retained: hsa-miR-21-5p ($cor = -0.29, p = 0.05$), hsa-miR-1236-3p ($cor = -0.4, p = 0.007$), and hsa-miR-3916 ($cor = -0.41, p = 0.005$) were the predicted miRNAs, and the correlation results were shown in Figure 6C. We then used four miRNAs to predict lncRNAs in the starbase database and intersected the results to obtain the lncRNA of hsa-miR-21-5p, and kept one lncRNA with negative correlation: MIR17HG ($cor = -0.31, p = 0.04$) (Figure 6D). The constructed ceRNA network was shown in Figure 6E. The lncRNA-miRNA-mRNA-drug was constructed based on the potential therapeutic drugs

identified in the previous step (Figure 6F). We found that lncRNA MIR17HG could regulate OSR1 by binding to hsa-miR-21-5p and that PAX2, EGLN1, and VHL might treat VV by targeting OSR1, CTNBN1, IGF1, LRP5, WNT2, HDAC1 by targeting WISP2, and STK4, CBF, STK3, and DBI by targeting CRIP1.

Quantitative real-time polymerase chain reaction validation

To further validate biomarker expression, we used qRT-PCR to compare the gene expression of WISP2, OSR1, and CRIP1 in diseased and normal venous vessels. The results showed that the expression of the WISP2 gene in diseased vessels was significantly upregulated, and that of OSR1 and CRIP1 genes in diseased vessels was significantly downregulated (Figure 7), as compared to normal samples.

Discussion

VV is a common peripheral vascular disease presenting twisted and dilated veins, usually in the lower extremities (Hamdan, 2012). Weakening of venous wall, valve dysfunction, and increased intravenous pressure are commonly considered to be its main causes (Hamdan, 2012). VV caused severe underlying vascular insufficiency including eczema, infection, venous ulceration, superficial thrombophlebitis, loss of subcutaneous tissue, and lipodermatosclerosis (Hamdan, 2012; Raffetto et al., 2020). Therefore, early identification of high-risk factors in VV patients

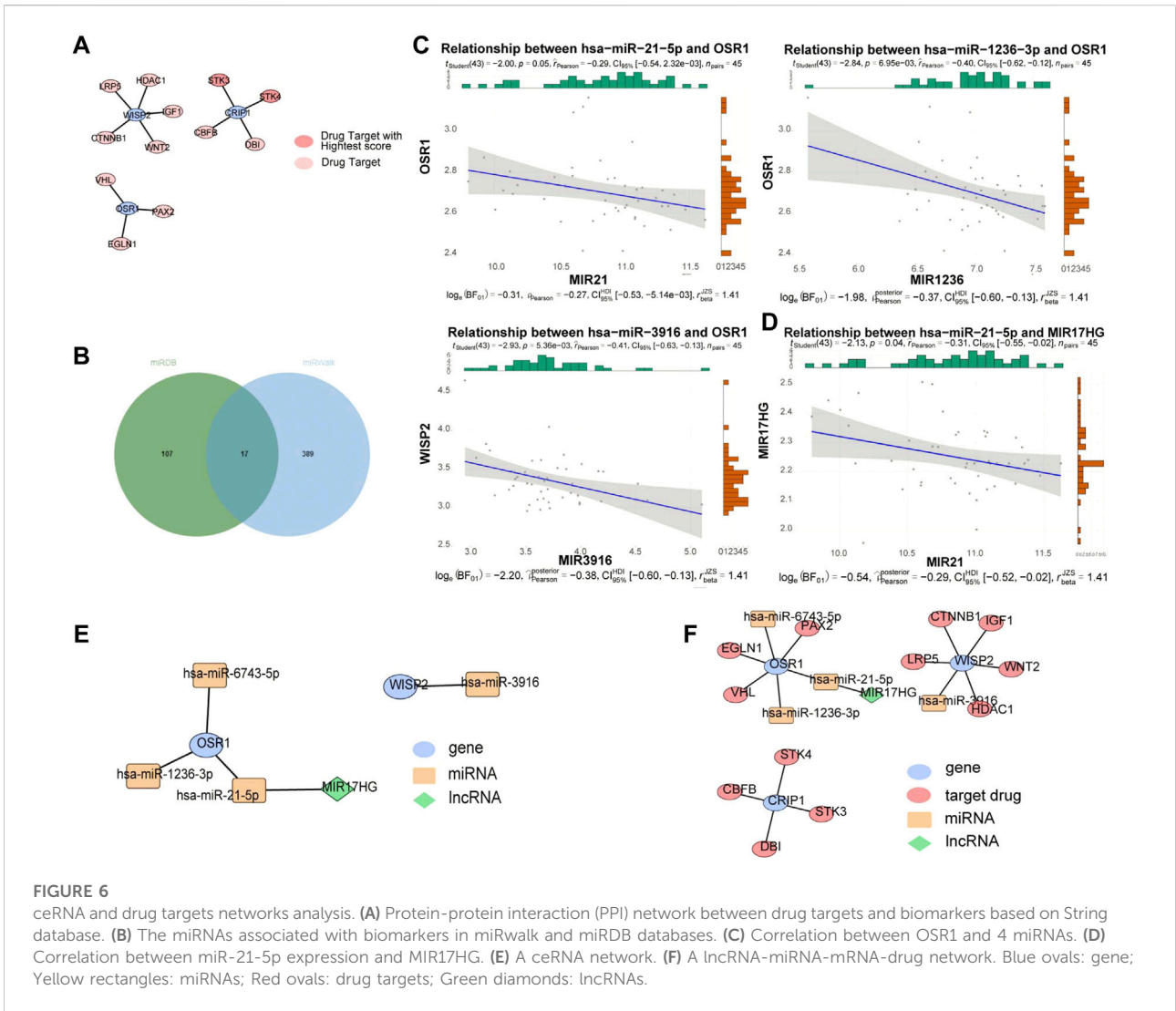


FIGURE 6

ceRNA and drug targets networks analysis. **(A)** Protein-protein interaction (PPI) network between drug targets and biomarkers based on String database. **(B)** The miRNAs associated with biomarkers in miRwalk and miRDB databases. **(C)** Correlation between OSR1 and 4 miRNAs. **(D)** Correlation between miR-21-5p expression and MIR17HG. **(E)** A ceRNA network. **(F)** A lncRNA-miRNA-mRNA-drug network. Blue ovals: gene; Yellow rectangles: miRNAs; Red ovals: drug targets; Green diamonds: lncRNAs.

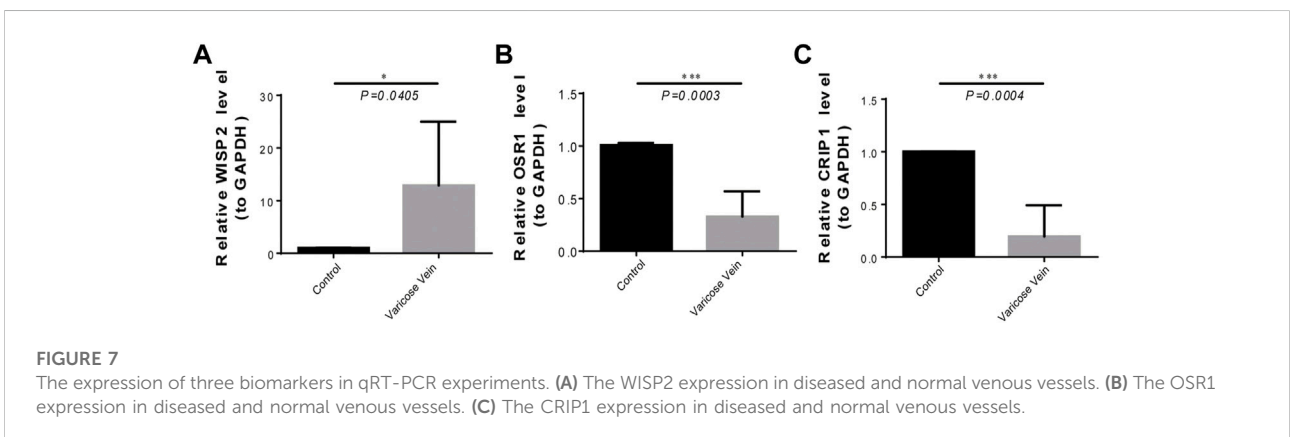


FIGURE 7

The expression of three biomarkers in qRT-PCR experiments. **(A)** The WISP2 expression in diseased and normal venous vessels. **(B)** The OSR1 expression in diseased and normal venous vessels. **(C)** The CRIP1 expression in diseased and normal venous vessels.

and early implementation of targeted preventive interventions will reduce the occurrence of VV and avoid wastage of healthcare resources.

In our study, three VV-MRGs, WISP2, CRIP1, and OSR1, were identified as potential biomarkers. Wnt1-inducible signaling pathway protein 2 (WISP2) is a secreted intracellular protein that is cell-specific and multifunctional (Hammarstedt et al., 2013; Grünberg et al., 2014). That WISP2 has been reported to be possibly regulated by the typical Wnt and TGF- β pathways for treatment of obesity and metabolic diseases, and developing new therapeutic strategies (Grünberg et al., 2018). In addition, it is regulated by the Wnt signaling pathway and IGF-1 to improve the metabolic status of animals (Alami and Liu, 2021). It can promote several types of tumors; for example, ovarian cancer cell proliferation by targeting ERK and YAP (Shi et al., 2020). However, the role of WISP2 in VV has not been previously reported, and we speculate that it may regulate VV through the Wnt signaling pathway. As an intracellular protein, WISP2 has been reported to be an important regulator of BMP4 action.

Cysteine-rich intestinal protein 1 (CRIP1), a LIM protein subfamily, contains a short LIM structural domain (Cai et al., 2017). CRIP1-positive circulating and splenic monocytes have been reported to play an important role in the inflammatory process associated with hypertension, and CRIP1 may influence the interaction of the immune system and the pathogenesis of hypertension (Schweigert et al., 2021). In addition, it can regulate the growth and differentiation of eukaryotic cells (Cai et al., 2017). Therefore, it is hypothesized that CRIP1 regulates VV through the immune system and inflammation.

Odd-skipped related 1 (OSR1) is an odd-skipped family zinc-finger protein (So and Danielian, 1999). OSR1 plays a vital role in heart and urogenital development, such as of kidneys and colon (Wang et al., 2005; Zhang and Jiang, 2020). In our study, it was found to play an important role in VV, suggesting that it can be a novel target for further studies.

GSEA showed that WISP2, CRIP1, and OSR1 are associated with oxidative phosphorylation, ECM, and respiratory system functions. Oxidative phosphorylation maintains homeostasis in all animals and plants (Wilson, 2017), and also plays an important role in vascular endothelial cells (ECs) (Li Q. et al., 2021). ECM remodeling processes regulate VV by venous hypertension (Barallobre-Barreiro et al., 2016). In addition, some respiratory system functions, such as pulmonary embolism (PE) has relationship with VV by venous thromboembolism (VTE) (Otero et al., 2013). Therefore, oxidative phosphorylation, extracellular matrix, and respiratory system might impact VV and provide new directions for further studies on VV.

Drug discovery is a time-consuming, costly, and complex process (Overington et al., 2006; Scannell et al., 2012). Reasonable drug target selection is an efficient strategy to reduce the risk of preclinical drug development

(Arrowsmith, 2011; Quan et al., 2018). In addition, promising and potentially high clinical efficacy drug targets have been identified, which is a key step in drug discovery (Dahlin et al., 2015). In this study, 12 drug targets, including IGF-1, VHL, CBF, and STK3, were identified by constructing PPI network between drug targets and biomarkers. Among them, it was shown that VHL was associated with elevated vascular endothelial growth factor (VEGF) concentration (Gordeuk et al., 2004). VHL mutations were associated with the development of vascular tumors, such as renal clear cell carcinoma, pheochromocytoma, pancreatic neuroendocrine tumors, and central nervous system hemangioblastoma. Moreover, IGF-1 factor was found to be associated with skin abnormalities, cause localized or diffuse hyperkeratotic plaques with or without hyperpigmentation, and increase the prevalence of VV and psoriasis (Sandru et al., 2021), which is consistent with our study. In addition, STK3 and STK4 are the top two drug targets in predicted drug targets. STK3/4 are important kinases in the Hippo signaling pathway (Cho et al., 2021). Their pharmacological inhibitors are reportedly effective in treatment of acute myeloid leukemia (Bata et al., 2022), and recent data indicate that they are potential therapeutic molecules for suppressing the Hippo signaling pathway, thereby improving tissue repair (Fan et al., 2016). However, their function in VV and contribution to its therapeutic molecules have not been investigated. To the best of our knowledge, CBF, LRP5, HDAC1, CTNBN1, WNT2, DBI, EGLN1, PAX2, STK3, and STK4 are the first reported drug targets in VV, and further experiments are needed to validate them.

By competitively binding to miRNA response elements (MREs) on mRNA, lncRNAs can cushion and restrain the protein expression of target mRNA, which is called the competitive endogenous RNA (ceRNA) mechanism. Studies have reported that ceRNA and drug target networks can provide effective and innovative therapeutic strategies for diseases. For example, analysis of ceRNA networks and identification of potential drug targets for drug-resistant leukemia cell K562/ADR (Liu et al., 2021), and ceRNA networks provide potential biomarkers and therapeutic targets for colorectal cancer (Wang et al., 2019), and in SARS-CoV-2 infection (COVID-19) (Arora et al., 2020). Therefore, it can provide novel and effective targets for the development of innovative therapeutic strategies against VV. In this study, lncRNA-miRNA-mRNA-drug network was built, and we found that lncRNA MIR17HG can regulate OSR1 by binding to hsa-miR-21-5p, and PAX2 might treat VV by targeting OSR1. Our study identified VV drug targets and their interrelations with miRNAs and lncRNAs; however, further studies are needed to provide new directions for its treatment.

In conclusion, WISP2, CRIP1, and OSR1 are possibly important biomarkers for VV diagnosis, exploration of potential molecular mechanisms, progression, and treatment. However, our study had some limitations. Statistically significant biomarkers were only determined by bioinformatics analysis in this study, but further validation, such as animal experiments and clinical trials is required. Some underlying mechanisms in VV require further investigation, such as gene knockdown and overexpression.

Data availability statement

Publicly available datasets (GSE68309, GSE68319, GSE36809) from GEO database were analyzed in this study. This data can be found in here: <https://www.ncbi.nlm.nih.gov/geo/>.

Ethics statement

The studies involving human participants were reviewed and approved by the Tianjin First Central Hospital Medical Ethics Committee. Written informed consent for participation was not required for this study in accordance with the national legislation and the institutional requirements.

Author contributions

SL and XL designed this study. SL and YL wrote the manuscript and performed bioinformatics analysis. ML and LW performed qRT-PCR experiments. SL, YL and XL revised the manuscript. ML and XL modified the language. All the authors have read and approved the final manuscript.

Acknowledgments

We thank all members of the GEO database for providing such a useful platform for researchers.

References

Alami, T., and Liu, J. L. (2021). Metabolic effects of CCN5/WISP2 gene deficiency and transgenic overexpression in mice. *Int. J. Mol. Sci.* 22 (24), 13418. doi:10.3390/ijms222413418

Arora, S., Singh, P., Dohare, R., Jha, R., and Ali Syed, M. (2020). Unravelling host-pathogen interactions: ceRNA network in SARS-CoV-2 infection (COVID-19). *Gene* 762, 145057. doi:10.1016/j.gene.2020.145057

Conflict of interest

The authors declare that the research was conducted in the absence of any commercial or financial relationships that could be construed as a potential conflict of interest.

Publisher's note

All claims expressed in this article are solely those of the authors and do not necessarily represent those of their affiliated organizations, or those of the publisher, the editors and the reviewers. Any product that may be evaluated in this article, or claim that may be made by its manufacturer, is not guaranteed or endorsed by the publisher.

Supplementary material

The Supplementary Material for this article can be found online at: <https://www.frontiersin.org/articles/10.3389/fgene.2022.1013803/full#supplementary-material>

SUPPLEMENTARY TABLE S1

DMCs between VV samples and normal samples of GSE68319 dataset.

SUPPLEMENTARY TABLE S2

DEGs between VV samples and normal samples of GSE68309 dataset.

SUPPLEMENTARY TABLE S3

Functional enrichment analysis of Methylation-Regulated Genes.

SUPPLEMENTARY TABLE S4

126 VVGs in brown module.

SUPPLEMENTARY TABLE S5

The GO enrichment analysis of WISP2.

SUPPLEMENTARY TABLE S6

The KEGG enrichment analysis of WISP2.

SUPPLEMENTARY TABLE S7

The GO enrichment analysis of CRIP1.

SUPPLEMENTARY TABLE S8

The KEGG enrichment analysis of CRIP1.

SUPPLEMENTARY TABLE S9

The GO enrichment analysis of OSR1.

SUPPLEMENTARY TABLE S10

The KEGG enrichment analysis of OSR1.

Arrowsmith, J. (2011). Trial watch: Phase II failures: 2008-2010. *Nat. Rev. Drug Discov.* 10 (5), 328–329. doi:10.1038/nrd3439

Bachman, J. (2013). Reverse-transcription PCR (RT-PCR). *Methods Enzymol.* 530, 67–74. doi:10.1016/b978-0-12-420037-1.00002-6

Barallobre-Barreiro, J., Oklu, R., Lynch, M., Fava, M., Baig, F., Yin, X., et al. (2016). Extracellular matrix remodelling in response to venous hypertension: Proteomics of human varicose veins. *Cardiovasc. Res.* 110 (3), 419–430. doi:10.1093/cvr/cvw075

- Bata, N., Chaikuad, A., Bakas, N. A., Limpert, A. S., Lambert, L. J., Sheffler, D. J., et al. (2022). Inhibitors of the Hippo pathway kinases STK3/MST2 and STK4/MST1 have utility for the treatment of acute myeloid leukemia. *J. Med. Chem.* 65 (2), 1352–1369. doi:10.1021/acs.jmedchem.1c00804
- Beebe-Dimmer, J. L., Pfeifer, J. R., Engle, J. S., and Schottenfeld, D. (2005). The epidemiology of chronic venous insufficiency and varicose veins. *Ann. Epidemiol.* 15 (3), 175–184. doi:10.1016/j.annepidem.2004.05.015
- Cai, H., Chen, J., Liu, J., Zeng, M., Ming, F., Lu, Z., et al. (2017). CRIP1, a novel immune-related protein, activated by *Enterococcus faecalis* in porcine gastrointestinal epithelial cells. *Gene* 598, 84–96. doi:10.1016/j.gene.2016.11.009
- Chang, S. L., Huang, Y. L., Lee, M. C., Hu, S., Hsiao, Y. C., Chang, S. W., et al. (2018). Association of varicose veins with incident venous thromboembolism and peripheral artery disease. *Jama* 319 (8), 807–817. doi:10.1001/jama.2018.0246
- Cho, Y. K., Son, Y., Saha, A., Kim, D., Choi, C., Kim, M., et al. (2021). STK3/STK4 signalling in adipocytes regulates mitophagy and energy expenditure. *Nat. Metab.* 3 (3), 428–441. doi:10.1038/s42255-021-00362-2
- Conway, J. R., Lex, A., and Gehlenborg, N. (2017). UpSetR: an R package for the visualization of intersecting sets and their properties. *Bioinformatics* 33 (18), 2938–2940. doi:10.1093/bioinformatics/btx364
- Dahlin, J. L., Inglese, J., and Walters, M. A. (2015). Mitigating risk in academic preclinical drug discovery. *Nat. Rev. Drug Discov.* 14 (4), 279–294. doi:10.1038/nrd4578
- Fan, F., He, Z., Kong, L. L., Chen, Q., Yuan, Q., Zhang, S., et al. (2016). Pharmacological targeting of kinases MST1 and MST2 augments tissue repair and regeneration. *Sci. Transl. Med.* 8 (352), 352ra108. doi:10.1126/scitranslmed.aaf2304
- Floyd, C., Ni, H., Gunaratne, R. S., Erban, R., and Papoian, G. A. (2022). On stretching, bending, shearing, and twisting of actin filaments I: Variational models. *J. Chem. Theory Comput.* 18 (8), 4865–4878. doi:10.1021/acs.jctc.2c00318
- Friso, S., Pizzolo, F., Choi, S. W., Guarini, P., Castagna, A., Ravagnani, V., et al. (2008). Epigenetic control of 11 beta-hydroxysteroid dehydrogenase 2 gene promoter is related to human hypertension. *Atherosclerosis* 199 (2), 323–327. doi:10.1016/j.atherosclerosis.2007.11.029
- Fukaya, E., Flores, A. M., Lindholm, D., Gustafsson, S., Zanetti, D., Ingelsson, E., et al. (2018). Clinical and genetic determinants of varicose veins. *Circulation* 138 (25), 2869–2880. doi:10.1161/circulationaha.118.035584
- Gloviczki, P., Comerota, A. J., Dalsing, M. C., Eklof, B. G., Gillespie, D. L., Gloviczki, M. L., et al. (2011). The care of patients with varicose veins and associated chronic venous diseases: Clinical practice guidelines of the society for vascular surgery and the American venous forum. *J. Vasc. Surg.* 53, 2S–48S. doi:10.1016/j.jvs.2011.01.079
- Gordeuk, V. R., Sergueeva, A. I., Miasnikova, G. Y., Okhotin, D., Voloshin, Y., Choyke, P. L., et al. (2004). Congenital disorder of oxygen sensing: Association of the homozygous Chuvash polycythemia VHL mutation with thrombosis and vascular abnormalities but not tumors. *Blood* 103 (10), 3924–3932. doi:10.1182/blood-2003-07-2535
- Grünberg, J. R., Elvin, J., Paul, A., Hedjazifar, S., Hammarstedt, A., and Smith, U. (2018). CCN5/WISP2 and metabolic diseases. *J. Cell Commun. Signal.* 12 (1), 309–318. doi:10.1007/s12079-017-0437-z
- Grünberg, J. R., Hammarstedt, A., Hedjazifar, S., and Smith, U. (2014). The novel secreted adipokine WNT1-inducible signaling pathway protein 2 (WISP2) is a mesenchymal cell activator of canonical WNT. *J. Biol. Chem.* 289 (10), 6899–6907. doi:10.1074/jbc.M113.511964
- Hamdan, A. (2012). Management of varicose veins and venous insufficiency. *Jama* 308 (24), 2612–2621. doi:10.1001/jama.2012.111352
- Hammarstedt, A., Hedjazifar, S., Jenndahl, L., Gogg, S., Grünberg, J., Gustafson, B., et al. (2013). WISP2 regulates preadipocyte commitment and PPAR γ activation by BMP4. *Proc. Natl. Acad. Sci. U. S. A.* 110 (7), 2563–2568. doi:10.1073/pnas.1211255110
- Hao, Z., Lv, D., Ge, Y., Shi, J., Weijers, D., Yu, G., et al. (2020). RIdeogram: Drawing SVG graphics to visualize and map genome-wide data on the ideograms. *PeerJ. Comput. Sci.* 6, e251. doi:10.7717/peerj-cs.251
- Huang, T., Zheng, Y., Qi, Q., Xu, M., Ley, S. H., Li, Y., et al. (2015). DNA methylation variants at HIF3A locus, B-vitamin intake, and long-term weight change: Gene-diet interactions in two U.S. Cohorts. *Diabetes* 64 (9), 3146–3154. doi:10.2337/db15-0264
- Jiang, H., Lun, Y., Wu, X., Xia, Q., Zhang, X., Xin, S., et al. (2014). Association between the hypomethylation of osteopontin and integrin β 3 promoters and vascular smooth muscle cell phenotype switching in great saphenous varicose veins. *Int. J. Mol. Sci.* 15 (10), 18747–18761. doi:10.3390/ijms151018747
- Kourou, K., Exarchos, T. P., Exarchos, K. P., Karamouzis, M. V., and Fotiadis, D. I. (2015). Machine learning applications in cancer prognosis and prediction. *Comput. Struct. Biotechnol. J.* 13, 8–17. doi:10.1016/j.csbj.2014.11.005
- Kundu, S., and Peterson, C. L. (2009). Role of chromatin states in transcriptional memory. *Biochim. Biophys. Acta* 1790 (6), 445–455. doi:10.1016/j.bbagen.2009.02.009
- Langfelder, P., and Horvath, S. (2008). Wgcna: an R package for weighted correlation network analysis. *BMC Bioinforma.* 9, 559. doi:10.1186/1471-2105-9-559
- Li, J. H., Liu, S., Zhou, H., Qu, L. H., and Yang, J. H. (2014a). starBase v2.0: decoding miRNA-ceRNA, miRNA-ncRNA and protein-RNA interaction networks from large-scale CLIP-Seq data. *Nucleic Acids Res.* 42, D92–D97. doi:10.1093/nar/gkt1248
- Li, Q., Zhu, Z., Wang, L., Lin, Y., Fang, H., Lei, J., et al. (2021a). Single-cell transcriptome profiling reveals vascular endothelial cell heterogeneity in human skin. *Theranostics* 11 (13), 6461–6476. doi:10.7150/thno.54917
- Li, W. H., Han, J. R., Ren, P. P., Xie, Y., and Jiang, D. Y. (2021b). Exploration of the mechanism of Zisheng Shenqi decoction against gout arthritis using network pharmacology. *Comput. Biol. Chem.* 90, 107358. doi:10.1016/j.compbiolchem.2020.107358
- Li, X., Jiang, X. Y., Ge, J., Wang, J., Chen, G. J., Xu, L., et al. (2014b). Aberrantly expressed lncRNAs in primary varicose great saphenous veins. *PLoS One* 9 (1), e86156. doi:10.1371/journal.pone.0086156
- Ling, C., and Groop, L. (2009). Epigenetics: A molecular link between environmental factors and type 2 diabetes. *Diabetes* 58 (12), 2718–2725. doi:10.2337/db09-1003
- Liu, Y., Chen, H., Hao, J., Li, Z., Hou, T., and Hao, H. (2020). Characterization and functional prediction of the microRNAs differentially expressed in a mouse model of concanavalin A-induced autoimmune hepatitis. *Int. J. Med. Sci.* 17 (15), 2312–2327. doi:10.7150/ijms.47766
- Liu, Z., Wang, Y., Xu, Z., Yuan, S., Ou, Y., Luo, Z., et al. (2021). Analysis of ceRNA networks and identification of potential drug targets for drug-resistant leukemia cell K562/ADR. *PeerJ* 9, e11429. doi:10.7717/peerj.11429
- Lynch, C. J., and Liston, C. (2018). New machine-learning technologies for computer-aided diagnosis. *Nat. Med.* 24 (9), 1304–1305. doi:10.1038/s41591-018-0178-4
- Mangiola, S., Doyle, M. A., and Papenfuss, A. T. (2021). Interfacing Seurat with the R tidy universe. *Bioinformatics* 37 (22), 4100–4107. doi:10.1093/bioinformatics/btab404
- Otero, R., Elias, T., Jara, L., Trujillo-Santos, J., Bertoletti, L., Nauffal, D., et al. (2013). Factors associated with elevated pulmonary arterial pressure levels on the echocardiographic assessment in patients with prior pulmonary embolism. *Thromb. Res.* 131 (5), e191–e195. doi:10.1016/j.thromres.2013.01.034
- Overington, J. P., Al-Lazikani, B., and Hopkins, A. L. (2006). How many drug targets are there? *Nat. Rev. Drug Discov.* 5 (12), 993–996. doi:10.1038/nrd2199
- Qin, J., Ke, J., Xu, J., Wang, F., Zhou, Y., Jiang, Y., et al. (2015). Downregulation of microRNA-132 by DNA hypermethylation is associated with cell invasion in colorectal cancer. *Oncol. Targets. Ther.* 8, 3639–3648. doi:10.2147/ott.S91560
- Qiu, X., Huang, F., Li, Z., Wei, X., Wu, J., Huang, J., et al. (2022). Develop a novel nomogram to predict respiratory failure in acute pancreatitis at early stage. *Clin. Lab.* 68 (4). doi:10.7754/Clin.Lab.2021.210826
- Qu, J., Li, B., Qiu, M., Wang, J., Chen, Z., Li, K., et al. (2022). Discovery of immune-related diagnostic biomarkers and construction of diagnostic model in varies polycystic ovary syndrome. *Arch. Gynecol. Obstet.* 306 (5), 1607–1615. doi:10.1007/s00404-022-06686-y
- Quan, Y., Wang, Z. Y., Chu, X. Y., and Zhang, H. Y. (2018). Evolutionary and genetic features of drug targets. *Med. Res. Rev.* 38 (5), 1536–1549. doi:10.1002/med.21487
- Raetz, J., Wilson, M., and Collins, K. (2019). Varicose veins: Diagnosis and treatment. *Am. Fam. Physician* 99 (11), 682–688.
- Raffetto, J. D., Ligi, D., Maniscalco, R., Khalil, R. A., and Mannello, F. (2020). Why venous leg ulcers have difficulty healing: Overview on pathophysiology, clinical consequences, and treatment. *J. Clin. Med.* 10 (1), E29. doi:10.3390/jcm10010029
- Robin, X., Turck, N., Hainard, A., Tiberti, N., Lisacek, F., Sanchez, J. C., et al. (2011). pROC: an open-source package for R and S+ to analyze and compare ROC curves. *BMC Bioinforma.* 12, 77. doi:10.1186/1471-2105-12-77
- Robinson, M. D., McCarthy, D. J., and Smyth, G. K. (2010). edgeR: a Bioconductor package for differential expression analysis of digital gene expression data. *Bioinformatics* 26 (1), 139–140. doi:10.1093/bioinformatics/btp616
- Sandru, F., Popa, A., Paduraru, D. N., Filipescu, A., Carsote, M., and Ghemigian, A. (2021). Skin anomalies in acromegalic patients (Review of the practical aspects). *Exp. Ther. Med.* 22 (5), 1330. doi:10.3892/etm.2021.10765

- Scannell, J. W., Blanckley, A., Boldon, H., and Warrington, B. (2012). Diagnosing the decline in pharmaceutical R&D efficiency. *Nat. Rev. Drug Discov.* 11 (3), 191–200. doi:10.1038/nrd3681
- Schweigert, O., Adler, J., Längst, N., Aissi, D., Duque Escobar, J., Tong, T., et al. (2021). CRIP1 expression in monocytes related to hypertension. *Clin. Sci.* 135 (7), 911–924. doi:10.1042/cs20201372
- Seok, J. (2015). Evidence-based translation for the genomic responses of murine models for the study of human immunity. *PLoS One* 10 (2), e0118017. doi:10.1371/journal.pone.0118017
- Shannon, P., Markiel, A., Ozier, O., Baliga, N. S., Wang, J. T., Ramage, D., et al. (2003). Cytoscape: A software environment for integrated models of biomolecular interaction networks. *Genome Res.* 13 (11), 2498–2504. doi:10.1101/gr.1239303
- Shi, Z. Q., Chen, Z. Y., Han, Y., Zhu, H. Y., Lyu, M. D., Zhang, H., et al. (2020). WISP2 promotes cell proliferation via targeting ERK and YAP in ovarian cancer cells. *J. Ovarian Res.* 13 (1), 85. doi:10.1186/s13048-020-00687-8
- Smetanina, M. A., Kel, A. E., Sevost'ianova, K. S., Maiborodin, I. V., Shevela, A. I., Zolotukhin, I. A., et al. (2018). DNA methylation and gene expression profiling reveal MFAP5 as a regulatory driver of extracellular matrix remodeling in varicose vein disease. *Epigenomics* 10 (8), 1103–1119. doi:10.2217/epi-2018-0001
- So, P. L., and Danielian, P. S. (1999). Cloning and expression analysis of a mouse gene related to *Drosophila* odd-skipped. *Mech. Dev.* 84 (1-2), 157–160. doi:10.1016/s0925-4773(99)00058-1
- Subramanian, A., Tamayo, P., Mootha, V. K., Mukherjee, S., Ebert, B. L., Gillette, M. A., et al. (2005). Gene set enrichment analysis: A knowledge-based approach for interpreting genome-wide expression profiles. *Proc. Natl. Acad. Sci. U. S. A.* 102 (43), 15545–15550. doi:10.1073/pnas.0506580102
- Tian, Y., Morris, T. J., Webster, A. P., Yang, Z., Beck, S., Feber, A., et al. (2017). ChAMP: Updated methylation analysis pipeline for illumina BeadChips. *Bioinformatics* 33 (24), 3982–3984. doi:10.1093/bioinformatics/btx513
- Turunen, M. P., Aavik, E., and Ylä-Herttua, S. (2009). Epigenetics and atherosclerosis. *Biochim. Biophys. Acta* 1790 (9), 886–891. doi:10.1016/j.bbagen.2009.02.008
- von Mering, C., Huynen, M., Jaeggi, D., Schmidt, S., Bork, P., and Snel, B. (2003). STRING: A database of predicted functional associations between proteins. *Nucleic Acids Res.* 31 (1), 258–261. doi:10.1093/nar/gkg034
- Wang, H., and Huang, G. (2011). Application of support vector machine in cancer diagnosis. *Med. Oncol.* 28, S613–S618. doi:10.1007/s12032-010-9663-4
- Wang, L., Cho, K. B., Li, Y., Tao, G., Xie, Z., and Guo, B. (2019). Long noncoding RNA (lncRNA)-Mediated competing endogenous RNA networks provide novel potential biomarkers and therapeutic targets for colorectal cancer. *Int. J. Mol. Sci.* 20 (22), E5758. doi:10.3390/ijms20225758
- Wang, L., Wang, Y., Liu, J., and Zhao, W. (2022). Identification of important genes of keratoconus and construction of the diagnostic model. *Genet. Res.* 2022, 5878460. doi:10.1155/2022/5878460
- Wang, Q., Lan, Y., Cho, E. S., Maltby, K. M., and Jiang, R. (2005). Odd-skipped related 1 (Odd 1) is an essential regulator of heart and urogenital development. *Dev. Biol.* 288 (2), 582–594. doi:10.1016/j.ydbio.2005.09.024
- Wang, Y., Xu, Y., Yang, Z., Liu, X., and Dai, Q. (2021). Using recursive feature selection with random forest to improve protein structural class prediction for low-similarity sequences. *Comput. Math. Methods Med.* 2021, 5529389. doi:10.1155/2021/5529389
- Wilson, D. F. (2017). Oxidative phosphorylation: Regulation and role in cellular and tissue metabolism. *J. Physiol.* 595 (23), 7023–7038. doi:10.1113/jp273839
- Xiao, W., Mindrinos, M. N., Seok, J., Cuschieri, J., Cuenca, A. G., Gao, H., et al. (2011). A genomic storm in critically injured humans. *J. Exp. Med.* 208 (13), 2581–2590. doi:10.1084/jem.20111354
- Yang, S., Wang, Y., Chen, Y., and Dai, Q. (2020). Masq: Next generation sequencing assists third generation sequencing for quality control in N6-methyladenine DNA identification. *Front. Genet.* 11, 269. doi:10.3389/fgene.2020.00269
- Yang, Z., Yi, W., Tao, J., Liu, X., Zhang, M. Q., Chen, G., et al. (2022). HPVMD-C: A disease-based mutation database of human papillomavirus in China. *Database.* Oxford. doi:10.1093/database/baac018
- Yu, G., Wang, L. G., Han, Y., and He, Q. Y. (2012). clusterProfiler: an R package for comparing biological themes among gene clusters. *Omics* 16 (5), 284–287. doi:10.1089/omi.2011.0118
- Zhang, F., and Jiang, Z. (2020). Downregulation of OSR1 promotes colon adenocarcinoma progression via FAK-mediated akt and MAPK signaling. *Oncotargets Ther.* 13, 3489–3500. doi:10.2147/ott.S242386
- Zhang, Z., and Wang, C. (2022). Exploring key genes and pathways of cardiac hypertrophy based on bioinformatics. *Dis. Markers* 2022, 2081590. doi:10.1155/2022/2081590